

Fortified chocolate mousse with powder and extract from *Moringa oleifera* leaves for nutritional value improvement

Olívia J.S. Gomes^a, Anabela Leitão^b, Marisa C. Gaspar^{c,d}, Carla Vitorino^{e,f}, João J.S. Sousa^{e,f}, Hermínio C. de Sousa^a, Mara E.M. Braga^{a,*}, Licínio M. Gando-Ferreira^{a,*}

^a University of Coimbra, CIEPQPF, Department of Chemical Engineering, Faculty of Sciences and Technology, Pólo II, Rua Sílvio Lima, 3030-790 Coimbra, Portugal

^b LESRA–Laboratory of Separation, Reaction and Environmental Engineering, Faculty of Engineering, Agostinho Neto University, Av. Ho Chimin no 201, Luanda, Angola

^c Centre for Innovative Care and Health Technology (ciTechCare), Polytechnic Institute of Leiria, 2410-541 Leiria, Portugal

^d ESSLeI–School of Health Sciences, Polytechnic Institute of Leiria, 2411-901 Leiria, Portugal

^e Faculty of Pharmacy, University of Coimbra, Pólo das Ciências da Saúde, Azinhaga de Santa Comba, 3000-548 Coimbra, Portugal

^f Coimbra Chemistry Centre, Institute of Molecular Sciences-IMS, Department of Chemistry, University of Coimbra, Rua Larga, 3004-535 Coimbra, Portugal

ARTICLE INFO

Keywords:

Moringa oleifera leaves
Chemical characterisation
Solvent extraction
Chocolate mousse
Acceptability profile

ABSTRACT

This study focuses on the characterisation and incorporation of *Moringa oleifera* leaf powder (MOP) from Luanda (Angola) and its extract (MOE) in fortified chocolate mousse. Dark green (DG) leaves presented superior nutritional values compared to other leaves. DG contained a higher concentration of mineral salts (10 ± 1 mg/100 g of dry leaves), phenolic compounds (267 ± 4 mg GAE/g), vitamins (1.9 ± 0.2 mg/g of dry extract) and strong antioxidant capacity (IC_{50} , 115 ± 8 μ g/mL). Therefore, DG leaves were used to fortify the chocolate mousse. The leaves were prepared in three samples: control, 2 % MOP (w/w) and 2 % MOE (v/v). Textural and rheological analysis of chocolate mousse samples revealed a pseudoplastic profile for all samples, with decreased texture attributes and viscosity due to the incorporation. The sensory evaluation demonstrated that MOP and MOE samples presented 93 % and 88 % resemblance to the original product regarding general acceptance, respectively.

1. Introduction

The consumption of moringa leaves by humans has gained significant attention as a potential strategy to combat and prevent malnutrition. Childhood malnutrition and micronutrient deficiencies significantly contribute to global child mortality rates, accounting for up to 45 % of deaths in children under the age of 5 years old. Moreover, malnutrition poses long-term health risks, disturbs cognitive development, affects productivity and reduces future earning potential (Brar et al., 2022). UNICEF's 2023 report revealed alarming statistics, with 22.3 % and 6.8 % of children under 5 years old worldwide being stunted and wasted, respectively (UNICEF, 2023). The global prevalence of vitamin A deficiency, which affects approximately 33 % of children aged 5–69 months, leads to vision impairments, increased mortality due to measles and diarrhoea-related complications (Imdad et al., 2022). In addition to micronutrient intake during childhood, dietary fibre may enhance intestinal health and microbiome diversity, consequently influencing the prevalence and recovery from malnutrition (Iddrisu

et al., 2021).

Moringa oleifera, a deciduous tree of the Moringaceae family, originates in India and is widely cultivated across Asia, Africa and tropical Central America. *M. oleifera* offers abundant nutrients in its flowers, seeds, leaves and roots, effectively countering deficiency diseases in humans and animals. Moringa leaves are rich in vital vitamins such as A and C and essential minerals such as copper, chromium, manganese, zinc and magnesium. Prominent phenolics found in *M. oleifera* leaves include flavonoids (e.g. epicatechin, catechin, quercetin and kaempferol) and phenolic acids (e.g. gallic acid, chlorogenic acid and caffeic acid) (Pollini et al., 2020; Rocchetti et al., 2020; Vonghirundecha et al., 2022).

The potential for enhancing traditional food products through fortification with sustainable sources is apparent in the field of nutrition. The use of dried leaf powder offers a viable substitute to traditional sources such as milk and eggs, meeting the nutritional needs of vegans and vegetarians aiming for equal protein intake (Yang et al., 2023). The diverse components of the moringa plant provide a remarkable example

* Corresponding authors.

E-mail addresses: marabraga@eq.uc.pt (M.E.M. Braga), lferreira@eq.uc.pt (L.M. Gando-Ferreira).

<https://doi.org/10.1016/j.foodchem.2023.138338>

Received 25 October 2023; Received in revised form 26 December 2023; Accepted 28 December 2023

Available online 3 January 2024

0308-8146/© 2023 The Author(s). Published by Elsevier Ltd. This is an open access article under the CC BY-NC-ND license (<http://creativecommons.org/licenses/by-nc-nd/4.0/>).

of this, thereby facilitating its integration. In general, the incorporation of various plant components into food items such as bread (Ia, 2021), snacks (Zungu et al., 2020), dairy products (Zhang et al., 2019) and drinks (Abera et al., 2022) leads to an improvement in the nutritional quality of the product, including proteins, essential amino acids, minerals and fibre.

Dairy-based desserts, appealing to diverse consumer groups such as older adults and children, obtain their varied textures, flavours and appearances from a combination of dairy ingredients and stabilisers (Saunders, 2022). These attributes significantly shape product acceptability. The expansive dairy dessert market offers diverse options, with certain variants gaining popularity among health-conscious consumers. The industry's focus on incorporating functional ingredients aligns with the increased demand for such products. However, the absence of previous research on the incorporation of moringa leaves into chocolate mousse provides a valuable opportunity to address potential drawbacks, such as green pigmentation, organic odours and alterations in mechanical properties, potentially impacting the final acceptability of the culinary product (Trigo et al., 2023).

M. oleifera has received significant global attention due to the exponential surge in research publications on the subject in recent years. The number of publications increased 10-fold between 2010 and 2022, and this trend is forecast to continue in 2023. As expected, *M. oleifera* stands out as the most prevalent keyword, appearing in 1,083 co-occurrences (Fig. A1). Other notable keywords include 'Moringa' (120), 'antioxidants' (94), 'oxidative stress' (56), 'coagulation' (53), 'water treatment' (44), 'antioxidant activity' (39) and 'flavonoids' (31). The author consistently includes terms in their abstracts, highlighting the plant's broad research coverage across pharmacology, biochemistry, water treatment and environmental sciences (Xinyue et al., 2023).

Although many studies have examined the integration of moringa into different food products, a noticeable gap exists in exploring how they affect the physical properties and consumer acceptance of moringa leaf and extract-enriched chocolate mousse. To achieve this objective, a thorough analysis of the nutrient content of moringa leaves at various maturity stages is conducted, along with an evaluation of the chemical and bioactive profile of its ethanolic extract. Subsequently, the rheological, textural and acceptability of fortified chocolate mousse are evaluated while analysing the influence of incorporation.

2. Material and methods

2.1. Plant material

Small branches were collected from three 5-year-old *M. oleifera* trees grown in Luanda, Angola (8°57'24.9"S, 13°13'02.9"E), yielding fresh, mature leaves with distinct colour variations: dark green (DG), intermediate green (IG) and yellowish green (YG). After careful washing, the leaves were air-dried at approximately 30 °C. The leaves were dried for 2 weeks until they reached equilibrium weight. The dried leaves were ground into a consistent, fine powder using a coffee grinder. The resulting powder was stored in sealed bags to maintain its quality and protect it from light and moisture.

2.2. Soil collection and characterisation

The soil was collected at a depth of 15 cm around the area where the leaves were removed. The soil was homogenised and stored in plastic containers. To ensure that the sample was representative, it was successively reduced to 300 g using the opposite-quarters technique after drying and sieving. Aliquots were obtained from this sample for each of the following tests, except for the determination of metals, which was performed in triplicate based on methods described by Teixeira et al. (2017).

Determination of moisture—The moisture of the sample was determined by drying it in an oven at 105 °C for 1 h. Values are presented in

relative proportions (%).

Determination of pH and electrical conductivity—A suspension of 1:2.5 g/mL soil in distilled water was agitated manually and measured with an electrode after shaking for 1 h at 100 rpm (APHA et al., 2023).

Determination of alkalinity—A suspension of soil in distilled water (1:2.5 g/mL) was shaken for 2 h at 100 rpm. Subsequently, 60 mL of the supernatant was titrated with 0.02 N sulphuric acid until pH 4.5.

Determination of Kjeldahl nitrogen—1 g of soil and 8 g of the Kjeldahl catalyst (CuSO₄·5H₂O) were added to the digestion tube with 15 mL of concentrated sulphuric acid. The mixture was digested in a digestion block with a fume collector. After digestion, the sample was distilled and titrated with a 0.02 N sulphuric acid solution to quantify the Kjeldahl nitrogen (N) collected in boric acid.

Determination of potassium—2 g of soil sample was suspended in 40 mL of distilled water, shaken for 2 h at 100 rpm and filtered (Whatman filter no. 2). The filtrate was acidified, and the potassium content was determined using a flame photometer.

Determination of phosphorus—The acid ascorbic method, described by (APHA et al., 2023) was used to quantify the soluble phosphorus (P).

Determination of calcium and magnesium—4 g of soil sample was suspended in 50 mL of KCl 1 M solution (pH 7), mixed (5 min at 100 rpm) and filtered (Whatman filter no. 2). The filtrate obtained can be used to determine the amount of Ca and Mg present in the soil by using standard methods for water based on complexometric titration with EDTA (APHA et al., 2023).

Determination of organic carbon and organic matter—The organic matter of 1 g of soil was oxidised at 180 °C with a mixture of potassium dichromate and sulphuric acid (APHA et al., 2023). A conversion factor of 1.724 was used to convert organic carbon to organic matter, assuming that organic matter contains 58 % organic C.

Determination of metals—A suspension of 1 g of soil in 40 mL of acetic acid solution (0.11 M) was shaken for 16 h at ambient temperature. The solution was filtrated (0.45 µm) and analysed for metals using an atomic absorption spectrophotometer. The detection limits for Fe, Mn, Zn and Cu were 0.05, 0.01, 0.01 and 0.02 mg/L, respectively (Pueyo et al., 2001).

2.3. Characterisation of *M. oleifera* leaf powder

2.3.1. Determination of the colour scale of the samples

The colour attributes of the powder were examined in triplicate using a spectropolarimeter (Chroma Metre CR-400 colourimeter, Konica Minolta Sensing Inc., Sakai, Japan). The L*, a* and b* parameters were used to quantify the levels of lightness, greenness/redness and blueness/yellowness, respectively.

2.3.2. Particle size determination

The particle size distribution of the powdered material was analysed in triplicate using laser diffraction spectroscopy in a Malvern Masterizer 2000 (Malvern Instruments, Malvern, UK). Ethanol was used as a dispersing agent. The sample was stirred for 2 min at 2,800 rpm and subjected to ultrasound for 10 s at 30 s intervals. Obscuration was 29 % ± 7 %, according to the Mi theory of calculation. This preparation ensured accurate and reliable measurements of the particle sizes present in the samples.

2.3.3. Centesimal composition

Determination of moisture and ash—The moisture content of the sample was determined by drying it in an oven at 105 °C for 24 h and ash by calcinating it at 300 °C for 3 h and raising it to 600 °C for 9 h using a previously described method (AOAC International et al., 2010). Values are presented in relative proportions (%).

Determination of fibres—The crude fibre content was determined (AOAC International et al., 2010). The method consists of an acid hydrolysis reaction with a solution of H₂SO₄ 1.25 % (v/v) and basic hydrolysis with a solution of NaOH 1.25 % (v/v) to break the cell walls of

the plant matrix. Values are presented in relative proportions (%).

Determination of lipids—The total lipid content was determined with hexane P.A. and Soxhlet apparatus, according to the AOAC method (AOAC International et al., 2010). Values are presented in relative proportions (%).

Determination of proteins—0.5 g of dried ground leaves was digested in a Kjeldahl flask containing concentrated sulphuric acid and a catalyst pellet (Sultana, 2020). The mixture was heated at 400 °C for 2 h, cooled and diluted. Distillation of the solution was performed with sodium hydroxide, and the distillate was titrated using a standardised solution of 0.1 N HCl. The amount of nitrogen was calculated according to Equation (1). Subsequently, the percentage of nitrogen in the sample was multiplied by 5.58 to obtain the total crude protein.

$$\text{NPN (\%)} = \frac{(\text{TS} - \text{TB}) * \text{HCl concentration} * 0.014}{\text{Sample mass (g)}} * 100 \quad (1)$$

where TS is the volume consumed in the distillate titration (in mL), TB is the volume consumed in the blank titration (in mL) and the HCl concentration is 0.1 N.

Determination of mineral contents—The methodology described by Sultana (2020) to determine the mineral contents (Fe, Ca, Na, Mg, K and Zn) was also used for the levels of heavy metals (Cr, Ni, Cd and Pb). The analyses for the quantitative determination of the mineral content were conducted using the flame spectrophotometry method and in different dilutions ranging from 1:2 to 1:50, v/v.

GC-MS analysis of volatile compounds—1 g of each powdered sample was placed into a 100-mL glass vial without any solvent. Adsorption time was 30 min at 55 °C, and desorption time was 3 min at the injection port (250 °C). The separation was achieved on a DB5-MS fused silica capillary column (30 m × 0.25 mm, 0.25 μm; Agilent J&W Scientific, Santa Clara, CA, USA), using helium as the carrier gas (1 mL/min). The temperature programme included an isothermal hold at 50 °C for 5 min, followed by a temperature ramp of 10 °C/min up to 270 °C, where it was held for 5 min. Volatile identification was based on the comparison of the mass spectra of the substances with the data bank of Mass Spectra Libraries (NIST and Flavours and Fragrances of Natural and Synthetic Compounds, FFNSC2.L). Peak relative areas of detected compounds were used for semi-quantitative analysis and presented as relative area proportions (%).

2.4. Extraction of bioactive compounds from *M. oleifera* leaf powder

The hot bath extraction method employed in this study used a thermostatic stirred shaking bath (VWR, model VLSB18, USA). A solvent mixture comprising 50 % v/v ethanol in an aqueous solution was utilised for the extraction. The extractions were performed for 2 h at 50 °C ± 0.1 °C and 120 rpm. The solid-to-solvent ratio used during the extraction process was set at 1:200 (g/mL). Upon completion of the extractions, the resulting extract was subjected to centrifugation at 5,000 rpm for 15 min. The supernatant was carefully transferred to a volumetric flask and the ethanol was subsequently removed using a rotary evaporator (Büchi Rotavapor, model R-210, USA).

2.4.1. Characterisation of moringa extracts

Total phenolic content—Total phenolic content was determined (Vieitez et al., 2018). The absorbance was read at 750 nm in a JASCO Model V-530 spectrophotometer. The result was calculated from the gallic acid standard curve and expressed as mg GAE/g of dry extract.

Total flavonoid content—To determine the total flavonoid content, the method of León-Félix et al. (2017) was used. The absorbance was read at 510 nm in a spectrophotometer. The result was calculated from the catechin standard curve and expressed in mg/100 g of catechin equivalents (CE).

Antioxidant capacity—The antioxidant activity of the samples was evaluated using the 2,2-diphenyl-1-picrylhydrazyl (DPPH) assay

(Almeida et al., 2021) and 2,2'-azino-bis(3-ethylbenzothiazoline-6-sulphonic acid) (ABTS⁺) scavenging (Peñalver et al., 2022). The IC₅₀ values were determined at 517 nm and the scavenging activity at 734 nm.

Chlorophyll content—The main pigments analysed in a spectrophotometer are chlorophyll A (663 nm) and B (645 nm), according to the simplified method described by Pérez-Patricio et al. (2018). The content was calculated according to Equation (2) as follows:

$$\text{Chlorophyll A (mg/mL)} = 12.7 * A_{663} - 2.69 * A_{645}$$

$$\text{Chlorophyll B (mg/mL)} = 22.9 * A_{645} - 4.68 * A_{663} \quad (2)$$

where A₆₄₅ is the absorbance at 645 nm and A₆₆₃ is the absorbance at 663 nm. The total chlorophyll content is the sum of chlorophyll A and B.

Determination of polyphenolic compounds—The analysis was performed using an UFLC chromatograph system coupled with a DAD detector (SPDM20A, Shimadzu, Japan). Separation was performed on a Luna C18 Phenomenex column (250 mm × 4.6 mm, 5 μm) maintained at 33 °C. The mobile phase consisted of two solutions: A (1 % acetic acid in water) and B (1 % acetonitrile). A gradient elution method was used, varying the proportions of solutions A and B over specific time intervals. The injection volume was 10 μL, the flow rate was set at 0.5 mL/min and the UV detector wavelength was 270 nm. Calibration curves were prepared with 10 phenolic standards dissolved in methanol at concentrations ranging from 0.1 to 1.0 μg/mL and R² values exceeding 98 %. The analysis criteria were based on the retention time and spectrum of each compound (Abdel Shakour et al., 2023; Kashaninejad et al., 2021; Khalid et al., 2023).

Determination of water- and fat-soluble vitamins—The analysis was conducted using an UFLC-DAD chromatograph system (SPDM20A, Shimadzu, Japan). For the analysis of fat-soluble vitamins (vitamins A and E), a chromatographic method was used based on the literature (Garai, 2017). A reversed-phase C18 column (150 mm × 4 mm, 5 μm) was used with a mobile phase consisting of 95:5 methanol:water at a flow rate of 1 mL/min. As for the water-soluble vitamins (vitamins C and B complex—B₁, B₂ and B₉), they followed Seal et al.'s method (Seal et al., 2019). Vitamins C and B₁ were detected at 245 nm, whereas vitamins B₂ and B₉ were detected at 275 nm. A Luna C18 column Phenomenex (250 mm × 4.6 mm, 5 μm) was used, with the mobile phase consisting of aqueous trifluoroacetic acid (0.01 % v/v) (solvent A) and acetonitrile (solvent B). The injection volume for all samples was 10 μL. Calibration curves were prepared with concentrations ranging from 50 to 500 μg/mL and R² values > 98 %.

2.5. Chocolate mousse sample preparation and incorporation

A commercial mix of chocolate mousse from a local brand was prepared following the instructions on the package. The recommended serving sizes and proportions of chocolate mousse powder and commercial semi-skimmed UHT milk were followed. The mixture was vigorously whisked until a creamy and homogeneous consistency was achieved. This food product was selected due to its dark brown colour, which can mask the green colour of the moringa leaves and extract. To incorporate moringa leaf powder, its extract was made in specific proportions of 2 % powder (w/w) and 2 % aqueous extract (v/v). The samples were subsequently refrigerated at 4 °C for 4 h to ensure proper solidification and cooling. The control sample, without any incorporation, was also prepared.

2.5.1. Rheological analyses of fortified mousse

The rheological analyses were performed following the methodology described (Gomez-Betancur et al., 2020). A Haake model RS1 controlled stress rheometer equipped with a plate-plate sensor was used in conjunction with a temperature control recirculation bath (Haake Phoenix II). The rheometer used a plate-plate geometry with a diameter of 20 mm and a 1.4 mm gap. The testing temperature was precisely set at 5 °C ± 0.2 °C to ensure consistent and accurate measurements.

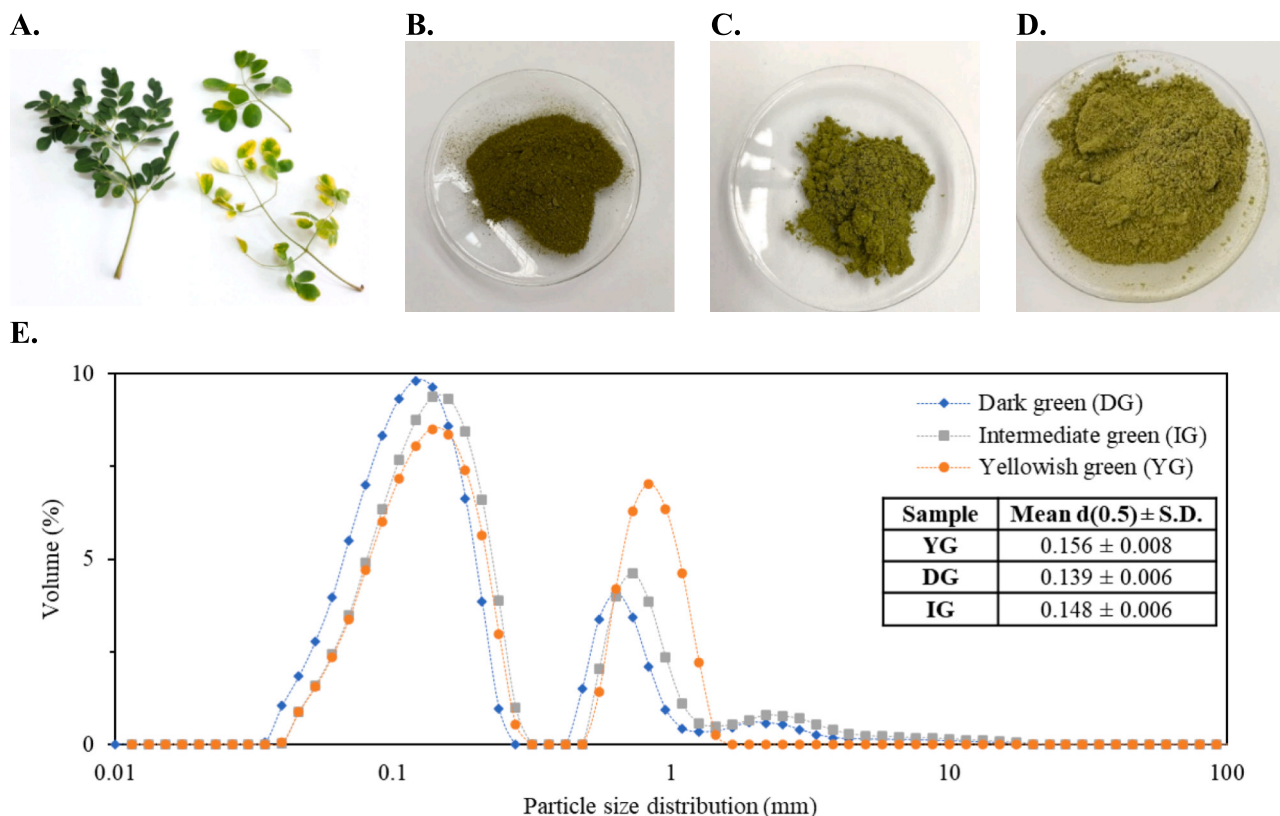


Fig. 1. *M. oleifera* leaves collected before grinding (A) and after in different colours: DG (B), IG (C), YG (D), and particle size distribution of the powder dispersed in ethanol in mm (E).

Large deformation analysis (flow profiles)—The flow profiles of the sample were measured using a three-phase analysis. First, an ascending curve ranging from 0 to 100 s^{-1} was measured for 1 min. This was followed by a holding time at a shear rate of 100 s^{-1} for 1 min. Finally, a descending curve from 100 to 0.01 s^{-1} was recorded for 1 min, following the methodology already described (Sah et al., 2016). The obtained data from the descending curve were fitted to the Herschel–Bulkley model (Equation (3)), providing an understanding of the sample's rheological properties under different shear rates.

$$\sigma = \sigma_0 + K \times \dot{\gamma}^n \quad (3)$$

where σ represents shear stress in Pascal (Pa), σ_0 represents yield stress in Pascal (Pa), K represents consistency index in Pascal seconds raised to the power of n ($\text{Pa} \cdot \text{s}^n$), $\dot{\gamma}$ represents shear rate in inverse seconds (s^{-1}) and n represents flow profile index.

To estimate thixotropy, the method followed was proposed by Soukoulis et al. (2010), using Equation (4) to analyse the ascending and descending curves of the apparent viscosity (η) and to determine the thixotropic profile as follows:

$$\text{Thixotropy}(\%) = 100 \times \frac{\eta - \eta'}{\eta} \quad (4)$$

where η and η' are the ascending and descending viscosities at 50 s^{-1} , respectively.

Small deformation analysis (static and dynamic measurements)—Following the previous methodology described by Gomez-Betancur et al. (2020), the linear viscosity range was defined beforehand using the least structured mousse by subjecting it to a strain spectrum (0.001 %–10 %) at a constant frequency of 1 Hz. Based on these findings, frequency sweeps were performed for all samples within the frequency range of 0.1–10 Hz, with a constant strain of 0.03 %. The G' and G'' moduli, as well as the phase displacement angle ($\delta = \arctan(G''/G')$),

were obtained from the resulting curve at 10 Hz (Lobato-Calleros et al., 2014). Creep compliance and recovery tests were conducted for 120 s each, applying a constant stress (σ) of 2 Pa. The elastic modulus (E_0), recovery percentage and liquid viscosity within the linear creep range (η_v) were obtained from the distinct curves obtained.

2.5.5.2. Instrumental analysis of texture

The textural characteristics of chocolate samples were evaluated instrumentally using a TA-XT Plus texture analyser (Stable Micro System Ltd., Surrey, UK). A 20-mm-diameter cylinder probe was depressed twice into the chocolate samples at a 5-mm/s rate up to a 10-mm depth, considering a trigger force of 5 g and a 15-s delay between the two consecutive compressions. For each sample, six measurements were performed. Data collection and analysis were conducted using the Texture Exponent 6.1.16.0 software package integrated into the instrument. The force–time curves provided valuable insights, enabling the determination of several mechanical parameters (Vitorino et al., 2013), as follows:

- (i) **Hardness**: the maximum peak force during the initial compression cycle;
- (ii) **Compressibility**: the work necessary to deform the sample in the first compression of the probe, extracted from the area under the force–time curve 1 (AUC₁);
- (iii) **Adhesiveness**: indicated by the negative force area for the first compression cycle, which corresponds to the work needed to overcome the attractive forces between the sample surface and the probe surface and is calculated from the area under the force–time curve 2 (AUC₂);
- (iv) **Cohesiveness**: the ratio of AUC₂ to AUC₁, with both compressions separated by a recovery period, providing insights into the internal structure of the sample;

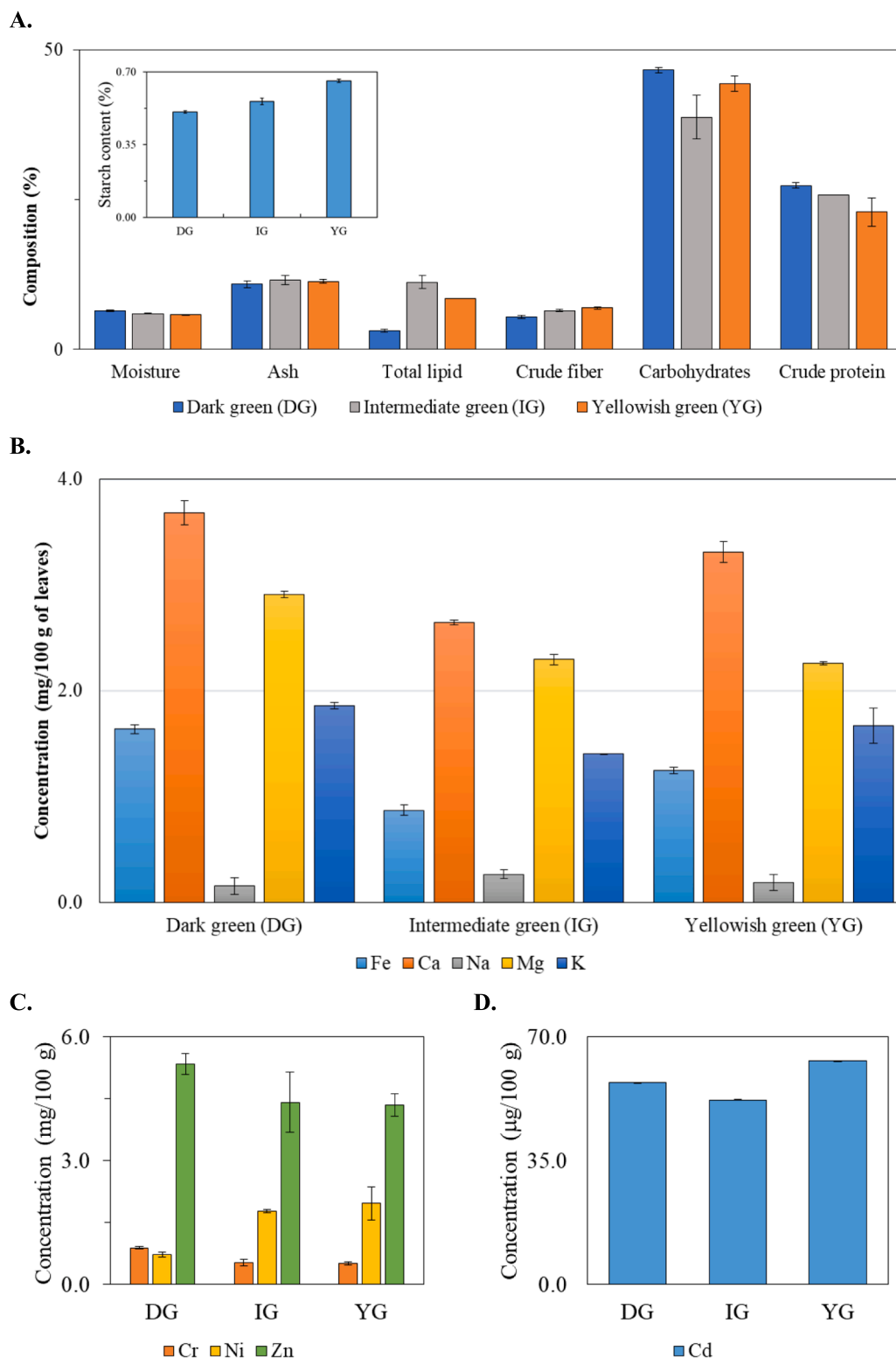


Fig. 2. Approximate composition (%) of powdered moringa leaves (A), mineral content mg/100 g (B) and heavy metal content in µg/100 g of dry leaves (C, D).

(v) **Elasticity**: the ratio of the time required to achieve maximum structural deformation on the second compression cycle to that on the first compression cycle.

2.6. Sensory acceptability profile

The sensory acceptability profile of the samples of interest was

evaluated using a scoring system ranging from 0 to 7 to rate the user acceptability of the product, with 0 suggesting extremely low acceptability and 7 suggesting extremely high acceptability. The selected attributes were colour, aroma, texture, flavour and general acceptance of the product. The control samples and mousse fortified with *M. oleifera* powder (2 % MOP, w/w) and leaf extract (2 % MOE, v/v) were randomly coded and evaluated by a panel of 36 participants, ages

Table 1

Extraction yield (% dry mass), total phenolic content (mg/g GAE dry weight), total flavonoid (mg/100 g CE) and antioxidant activity (DPPH, $\mu\text{g/mL}$ and ABTS, %) of different extracts of *M. oleifera* leaves. Results are expressed as mean \pm SD, $n = 3$.

Sample	Yield (%)	Total phenolic compounds (mg GAE/g of dry extract)	Total flavonoid (mg/100 g CE)	Antioxidant activity (IC ₅₀ , $\mu\text{g/mL}$)	ABTS (%scavenging activity)	Chlorophyll content (mg/100 g)
DG	38.27 \pm 0.04	267 \pm 4	317.5 \pm 12.3	115 \pm 8	40.1 \pm 0.3	250 \pm 11
IG	33.2 \pm 0.1	218.3 \pm 2.8	217.0 \pm 4	129 \pm 4	39.1 \pm 0.9	243 \pm 4
YG	30.22 \pm 0.02	213.5 \pm 4.9	207 \pm 3	212 \pm 13	35.9 \pm 0.3	241 \pm 11

Table 2

Quantification of vitamin A, complex B, C and E in powdered moringa leaves. Results are expressed as mean \pm SD, $n = 3$.

Vitamins	Retention time (min)	Vitamins ($\mu\text{g/g}$ of dry extract)		
		DG	IG	YG
A	3.54 \pm 0.01	504 \pm 17	410.6 \pm 14.8	439.5 \pm 15.5
C	7.9 \pm 0.2	11.18 \pm 2.36	6.5 \pm 1.4	4.9 \pm 0.4
B ₁	9.57 \pm 0.01	18.8 \pm 1.9	3.8 \pm 0.5	5.3 \pm 0.5
E	17.41 \pm 0.01	1349.2 \pm 47.4	1342 \pm 46	1022 \pm 35
B ₉	24 \pm 2	2.6 \pm 0.2	13.4 \pm 0.7	2.0 \pm 0.2
B ₂	27.06 \pm 0.01	25 \pm 2	1.87 \pm 0.74	3.63 \pm 0.65

Table 3

The intensity of the sensory attributes for mousse samples. Results are expressed as mean \pm SD, $n = 3$.

Sensory attributes	Control	MOP	MOE
Hardness (g)	152 \pm 15	116 \pm 4	58 \pm 7
Adhesiveness (g s)	-44 \pm 5	-25 \pm 4	-18 \pm 6
Springiness	1.00 \pm 0.04	0.9 \pm 0.1	0.8 \pm 0.1
Cohesiveness	0.53 \pm 0.02	0.49 \pm 0.03	0.41 \pm 0.02
Gumminess	80 \pm 7	56 \pm 3	24 \pm 2
Chewiness	80 \pm 6	48 \pm 8	18 \pm 4
Resilience	0.13 \pm 0.01	0.16 \pm 0.03	0.17 \pm 0.02

20–50, from the Department of Chemical Engineering, University of Coimbra, Portugal. Ethics approval was not required for this study. Participants were not coerced into participation, and a comprehensive disclosure of study requirements and risks was provided. Verbal consent was obtained from participants, and no release of participant data occurred without their knowledge.

2.7. Statistical analysis

Each experiment was conducted in triplicate. The results were expressed as mean \pm standard deviation and presented with significant figures. The experimental data underwent analysis of variance (ANOVA) using Analysis Tool Pak to perform Excel data analysis (Microsoft 365, Excel 2311, USA), and mean comparisons were conducted using the least significant difference at a 5 % level of significance.

3. Results and discussion

3.1. Soil characterisation

The determined values for soil properties are as follows: moisture at 0.87 % \pm 0.09 %, pH at 8.53 \pm 0.01, electrical conductivity at 20 \pm 1 $\mu\text{S/cm}$, alkalinity at 102.78 \pm 0.96 mg CaCO₃/L, potassium content at 634.9 \pm 5.7 mg/kg, phosphorus content at 15.4 \pm 0.6 mg/kg, calcium content at 678 \pm 4 mg/kg, magnesium content at 71.7 \pm 1.7 mg/kg, organic carbon at 3.87 \pm 0.08 mg/g, organic matter at 6.67 \pm 0.13 mg/g, iron content at 3.25 \pm 0.01 mg/kg, manganese content at 204 \pm 1

mg/kg, zinc content at 16.8 \pm 0.1 mg/kg and nitrogen and copper undetected. According to Adebayo (2017), the major nutrient content of this soil appears to be inadequate, with a high deficiency in nitrogen and an excess in potassium. The major nutrients N, P and K have significant effects on the growth of *M. oleifera* trees.

3.2. Characterisation of *M. oleifera* leaf powder

The colour parameters of the *M. oleifera* leaf powder are presented in Table A1. Higher L* values indicate greater light reflectance, suggesting the light colour characteristics of a product low in sugars or with the presence of starch (Zbikowska et al., 2022). The values of a* and b* indicate that the powder colour is leaning towards greenish or yellowish tones, showing the difference among the samples from the green tone being more intense (DG) to less intense (YG). The yellowish tone is a common indicator of nitrogen deficiency. Fig. 1A, B and C show the *M. oleifera* leaves collected before and after grinding at different stages of maturity: DG, IG and YG, respectively.

The study of particle size clarifies how grinding impacts extraction and mousse distribution. Fig. 1E demonstrates the bimodal distribution of the three sample types. As the powder particles have a low charge density, aggregation is expected. For this reason, the application of ultrasound within 30 s improved the disaggregation and maintained two well-defined families of distribution. The particle size range of the three samples was between 0.05 and 10 μm , and their median particle size (D₅₀) was lower for DG and higher for YG (from 0.14 to 0.16 μm , respectively).

Previous findings reported an increase in surface agglomerates in ultrafine water dropwort powders after grinding (Y. Zhang et al., 2022). This phenomenon is attributed to the enhanced electrostatic interactions resulting from the exposure of polar groups, leading to uneven powder distribution and an increased span value, from 5.06 \pm 0.03 (DG) to 5.35 \pm 0.07 (IG). Additionally, the reduction in particle size resulted in a significant increase in specific surface area, from 92.9 \pm 5.1 (YG) to 105.3 \pm 5.4 (DG) m²/kg, as reported by (Bullard et al., 2021). The decrease in particle size enables a higher particle count per unit weight, facilitating rapid incorporation and homogeneous blending with active food ingredients.

After the physical characterisation (colour and particle size), the chemical composition of moringa leaves was analysed according to macro-components (Fig. 2).

Fig. 2A shows that all parameters indicate a statistically significant difference among the values obtained for the three samples ($p < 0.05$) as determined by one-way ANOVA. The highest protein content (25.3 % \pm 4.5 %) was found in DG leaves. IG leaves presented the lowest carbohydrate contents (38.8 % \pm 3.6 %), of which 0.56 % \pm 0.02 % are starch. The lipid content in the samples was generally low, with IG leaves having the highest content (11.3 % \pm 1.1 %) and DG leaves having the lowest (3.2 % \pm 0.2 %). A low fibre quantity (between 5.43 % and 6.94 %) was observed. While appropriate crude fibre levels enhance digestibility and facilitate the absorption of microelements such as glucose and fat, their high content can lead to intestinal irritation, reduced digestibility and diminished nutrient utilisation (Sumczynski et al., 2023). The caloric value of each sample to DG (324 kcal), IG (360

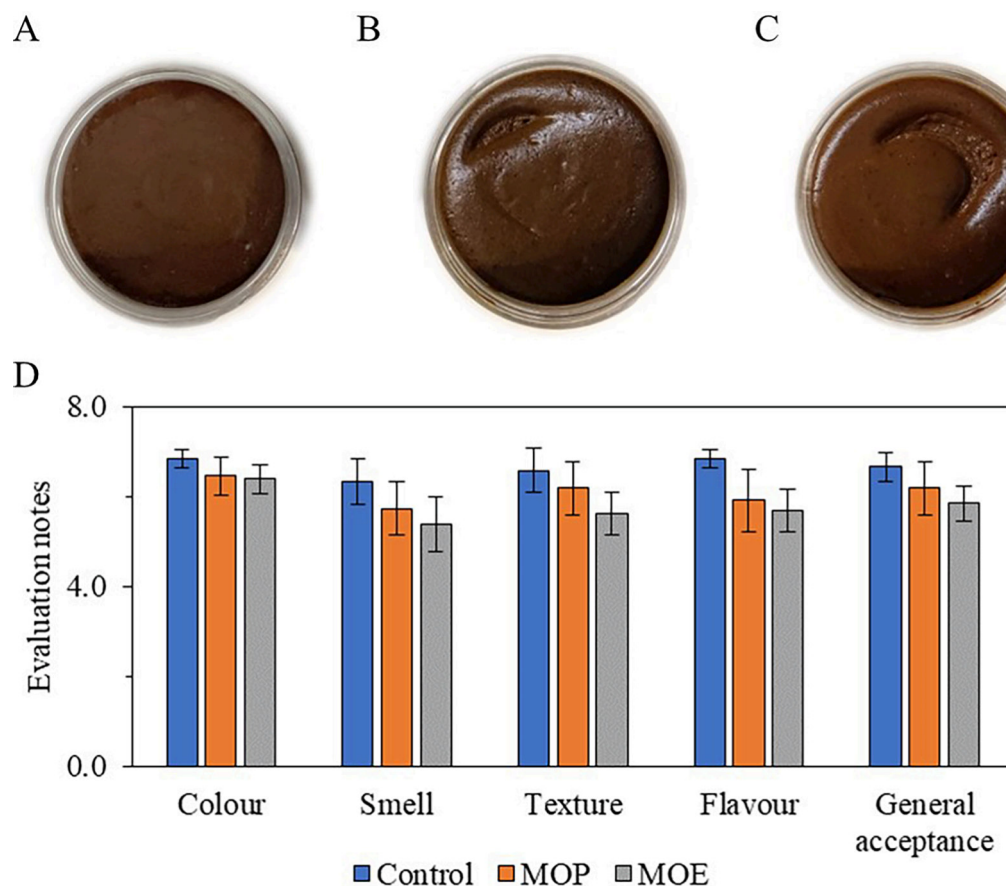
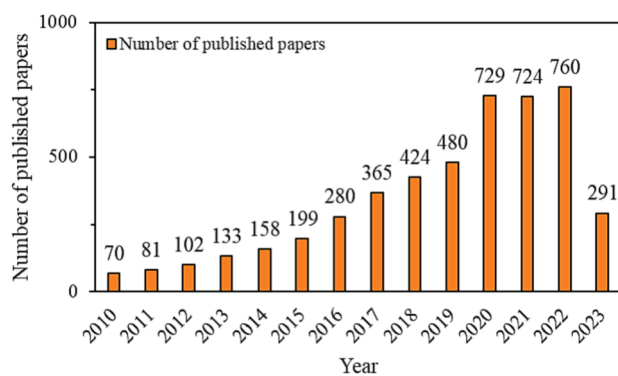


Fig. 3. Different mousse samples were prepared: control sample (A), fortified with 2% moringa leaf powder (2% MOP) (B), fortified with 2% moringa aqueous extract (2% MOE) (C) and sensory evaluation of chocolate mousse fortified with moringa leaves and extract.



Keywords	Frequency of occurrence
<i>Moringa oleifera</i>	1083
Moringa	120
Antioxidant	94
Oxidative stress	56
Coagulation	53
Water treatment	44
<i>Moringa oleifera Lam</i>	42
Antioxidant activity	39
Growth	38
Antioxidants	34

Fig. A1. Representation of the annual publication trends and frequencies of keywords in *M. oleifera* research (Xinyue Su et al., 2023).

kcal) and YG (346 kcal) was calculated by multiplying the values of the crude protein, lipid and carbohydrate by 3.99, 9.1, 3.99, respectively, and taking the sum of the product (Sultana, 2020).

The DG sample showed the highest concentrations of mineral salts, except for sodium (Fig. 2B). The comparative analysis highlighted significant variations in micronutrient levels among the three samples. In addition, chromium and zinc present expressive values regarding the other minerals (Fig. 2C), with the lowest amount of cadmium in DG leaves (Fig. 2D). The equipment detected no lead in the leaves at a level of < 0.03 ppm.

A general composition profile of the volatile compounds in three samples of *M. oleifera* leaves was analysed via GC-MS. The spectral data

of identified compounds were compared to those from NIST 98 (National Institute of Standards and Technology, Gaithersburg, MD, USA) and the Wiley 6.0 (Wiley, New York, NY, USA) library. A total of 32 volatiles were identified as common to all three samples (Table A3).

In the DG sample, 23 volatile compounds were identified. The most abundant volatile was 6-methyl-5-hepten-2-one (4.7 %), responsible for a citrus and fruity odour (Zhogoleva et al., 2023). Terpenes such as limonene (4.1 %), sabinene (0.6 %), pinene (0.5 %) and terpinene (0.5 %) were also noted. Other compounds included benzaldehyde (3.7 %), cyclocitral (an apocarotenoid) (3.6 %), 3,6-dimethyldecane (2.7 %) and hexalactone (1.6 %). The IG sample contained 30 identified compounds, with limonene being the most abundant (11.4 %). Other major

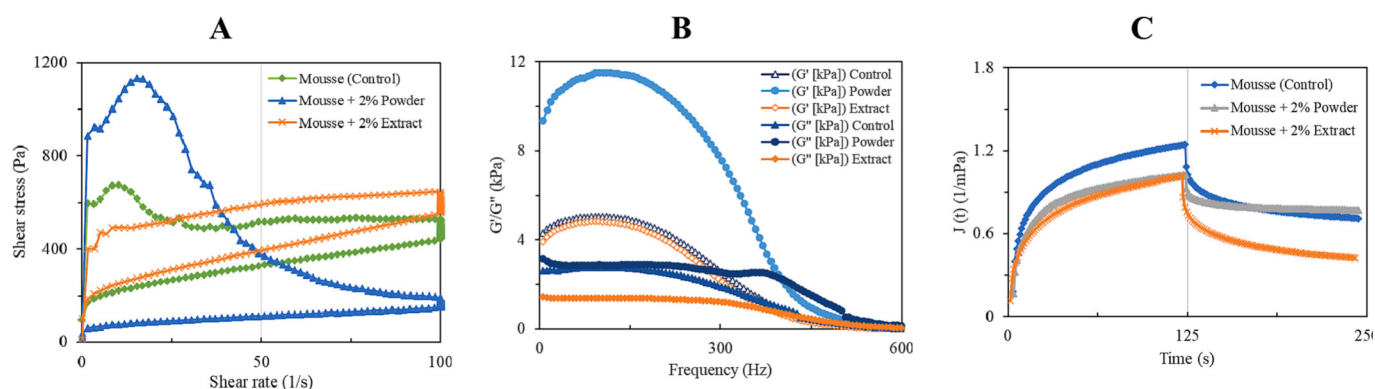


Fig. A2. Flow profile (A), frequency sweep [filled markers as storage modulus (G') and empty ones as loss modulus (G'')] (B) and creep compliance and recovery (C).

Table A1

Mean values of the Hunter scale parameters of moringa leaf powder.

Samples	L*	a*	b*
DG	56.97 ± 0.31	-5.06 ± 0.02	24.21 ± 0.01
IG	61.36 ± 0.28	-6.84 ± 0.01	28.23 ± 0.01
YG	62.43 ± 0.01	-5.09 ± 0.02	28.57 ± 0.01

Table A2

Contents of polyphenolic compounds ($\mu\text{g/g}$ of dry extract) in the moringa leaf powder. Results are expressed as mean \pm SD, n = 3.

Polyphenolic compounds	Compound class	Retention time (min)	Total compound ($\mu\text{g/g}$ of dry extract)		
			YG	DG	IG
Gallic acid	Phenolic acids	6.50 ± 0.53	31.82 ± 1.64	10.5 ± 0.6	25.97 ± 1.32
Catechin	Flavonoids	21.9 ± 1.0	88.94 ± 4.42	268.75 ± 13.48	103.74 ± 5.23
Epicatechin	Flavonoids	24.74 ± 0.09	51.74 ± 2.69	183.97 ± 9.25	59.14 ± 3.05
Caffeic acid	Phenolic acids	25.8 ± 0.2	0.63 ± 0.18	23.24 ± 1.30	0.66 ± 0.04
Vanillic acid	Phenolic acids	26.54 ± 0.08	0.94 ± 0.28	1.34 ± 0.16	0.75 ± 0.45
Syringic acid	Phenolic acids	27.39 ± 0.26	8.93 ± 0.44	127.7 ± 6.5	83.27 ± 4.29
Rutin	Flavonoids	29.4 ± 0.2	208.4 ± 10.5	274.87 ± 13.73	270.26 ± 13.57
Coumaric acid	Phenolic acids	32.4 ± 0.1	15.7 ± 0.9	2.7 ± 0.2	25.07 ± 1.36
Ferulic acid	Phenolic acids	33.4 ± 0.3	14.8 ± 0.8	153.8 ± 7.8	56.15 ± 2.85
Quercetin	Flavonoids	34.38 ± 0.05	27.1 ± 1.5	136.8 ± 6.9	105.3 ± 5.4

compounds in the IG sample were 2(3H)-furanone (6 %), 6-methyl-5-hepten-2-one (4.7 %), benzaldehyde (4.4 %), pinene (2.7 %), decane (2.1 %), nonanal (2.3 %) and benzene ethanol (2.3 %). In the YG sample, limonene was also the most abundant compound, accounting for 11.82 % of total volatiles. This was followed by 6-methyl-5-hepten-2-one (4.8 %), benzaldehyde (3.8 %), dodecane (2.7 %), hexadecane (2.6 %), hexalactone (2.3 %) and nonanal (2.2 %).

The differences in volatile compounds among the three *M. oleifera* samples could be attributed to variations in their main terpenes and fatty acid components. Ester-derived compounds (pentanoic, butanoic and octadecatrienoic acid) were particularly prevalent in the DG sample. In contrast, hydrocarbon-derived compounds (tridecane to undecane) were noticeably absent in the IG and YG samples.

Table A3

Comparison of volatile compounds in moringa leaves in different mature stages.

Compound	RT (min)	Area (%)		
		DG	IG	YG
Pentanoic acid	5.1	2.86 ± 0.06	-	-
Butanoic acid	5.6	1.5 ± 0.3	1 ± 0	-
2(3H)-furanone	7.0	1.3 ± 0.2	2.1 ± 0.7	1.3 ± 0.2
Pinene	7.4	-	1.6 ± 0.5	2 ± 0
Benzaldehyde	8.2	3.7 ± 0.2	4.4 ± 0.2	3.8 ± 0.3
6-Methyl-5-hepten-2-one	8.7	4.7 ± 0.2	4.8 ± 0.2	4.7 ± 0.9
Sabine	9.4	0.80 ± 0.02	0.5 ± 0.1	-
Terpinene	9.3	1.10 ± 0.05	1.0 ± 0.2	1.0 ± 0.2
Limonene	9.7	4.1 ± 0.8	11.4 ± 1.5	11.8 ± 1.5
Eucalyptol	9.7	0.69 ± 0.03	3.0 ± 0.9	3.0 ± 0.7
Benzene acetaldehyde	10.0	1.13 ± 0.06	1.91 ± 0.03	1.5 ± 0.2
Decane	10.5	2.7 ± 0.1	2.1 ± 0.1	1.3 ± 0.2
Nonanal	11.1	-	2.3 ± 0.2	2.2 ± 0.2
Cyclohexanol	11.3	1.78 ± 0.07	2 ± 0	-
Benzene ethanol	11.3	1.7 ± 0.3	2.3 ± 0.3	1.3 ± 0.3
Cyclopentasiloxane	11.5	1.2 ± 0.2	1.4 ± 0.2	1.1 ± 0.4
Benzene acetonitrile	11.8	1.3 ± 0.2	1.0 ± 0.2	0.7 ± 0.1
4-Ketoisophorone	12.1	-	1.5 ± 1	0.4 ± 0.1
Epoxylinolool	12.4	-	1.0 ± 0.3	0.8 ± 0.1
Dodecane	12.7	2.7 ± 0.3	2.5 ± 0.1	2.71 ± 0.06
Safranal	12.8	2.5 ± 0.4	2.3 ± 0.2	2.1 ± 0.4
Undecane	13.0	1.2 ± 0.1	1.1 ± 0.1	1.1 ± 0.2
Cyclocitral	13.1	3.6 ± 0.6	2.55 ± 0.08	2.2 ± 0.1
Dodecane	13.5	1.5 ± 0.2	1.6 ± 0.7	1.2 ± 0.2
Pentadecane	13.9	2.8 ± 0.2	2.2 ± 0.3	0.7 ± 0.1
Tetradecane	15.6	1.3 ± 0.3	-	1.3 ± 0.4
Hexacosane	14.1	-	1.3 ± 0.5	0.4 ± 0.1
Tridecane	14.2	1.3 ± 0.2	-	1.0 ± 0.2
Neryl acetone	16.3	-	2.7 ± 0.2	2.9 ± 0.8
Ionone	16.1	1.8 ± 0.5	-	-
3-Buten-2-one	16.7	0.8 ± 0.2	-	3.2 ± 0.3
2(4H)-benzofuranone	17.5	1.4 ± 0.5	2.3 ± 0.3	2.4 ± 0.9

3.3. Extraction and characterisation of *M. oleifera* leaf

Table 1 summarises the extraction yield (% dry mass), total phenolic content (mg GAE/g), total flavonoid (mg/100 g CE), antioxidant activity (DPPH, $\mu\text{g/mL}$ and ABTS, %) and chlorophyll content (mg/100 g) of leaf powder on the different 50 % ethanolic extracts.

The samples showed a significant difference ($P < 0.05$), except for scavenging activity by ABTS and chlorophyll content. The extraction

yield was highest for the DG sample compared to the other samples. This can be attributed to the smaller particle size and surface area of the DG leaf powder (Fig. 1E), resulting in higher levels of total phenolics, flavonoids and antioxidant activity (IC₅₀). The phenolic compound content was not notably different between the YG and IG samples, suggesting that the maturation (Fig. 1A–D) stage did not affect these compounds. However, the DG leaves exhibited the lowest antioxidant activity, possibly due to their richest polyphenol content. In contrast, the most mature leaves (YG and IG) showed similar antioxidant activity by IC₅₀. The ABTS⁺ free radical assay shows subtle similarities between DG and IG samples, but DG and YG display a significant difference, suggesting that antioxidant content may degrade with maturity.

The contents of the polyphenolic compounds in the leaves of a 50 % ethanol extract of moringa leaf powder were analysed by the UFLC system. The analysis of the polyphenolic compounds of the extracts is shown in Table A2. The DG extract exhibited the highest levels of catechin, (–) epicatechin, caffeic acid, vanillic acid, syringic acid, rutin and *t*-ferulic acid. In contrast, gallic acid, *p*-coumaric acid and quercetin showed similar levels in the IG and YG leaves. The higher concentration of these compounds in tender leaves aligns with their role in the plant's defence mechanism against reactive oxygen species. As the leaves mature, enzymatic processes may lead to the conversion of these compounds to other secondary metabolites, resulting in lower levels (Hasanuzzaman et al., 2020).

The strong antioxidant activity of the extracts can be attributed to the high concentration of phenolic compounds (also shown in Table 1). These compounds possess hydroxyl groups, which contribute to their scavenging ability (Platzer et al., 2022). The ingestion of up to 1 g of polyphenolic compounds from a diet rich in fruits and vegetables has been shown to prevent mutagenesis and carcinogenesis in humans (Trigo et al., 2023). Phenolic compounds, such as phenolic acids, flavonoids and phenylpropanoids, are known for their free radical scavenging and antioxidant activities, thus accounting for the significant antioxidant activity of *M. oleifera*. Each polyphenolic compound exhibits various biological activities. Catechin, epicatechin, rutin, ferulic acid and quercetin, present in significant amounts in moringa leaves, have demonstrated potent antioxidant, anti-inflammatory and anti-cancer properties (Bae et al., 2020).

The quantification of vitamin A, complex B, C and E in powdered moringa leaf extracts led to the concentration values shown in Table 2.

It is important to note that vitamin C is highly sensitive to temperature and may undergo degradation during the extraction process. Notably, it appears that DG has the highest concentration of water-soluble vitamins, possibly because the leaves' maturation would result in the degradation of most of them. Significant amounts of fat-soluble vitamins were also present in the DG samples. This could be due to the presence of crude lipids and/or higher protein content, which may be associated with the molecule and offer additional protection against thermal processes (Krakowska-Sieprawska et al., 2022).

3.4. Fortified chocolate mousse sample evaluation

Incorporating moringa compounds, such as leaf powder or extracts, in mousses will enhance their chemical profile by increasing their nutritional content. Among different types of moringa, DG powder presented superior chemical value (Fig. 2A) and higher concentrations of essential mineral salts, such as iron, calcium, magnesium and zinc (Fig. 2B). Additionally, the extracts have demonstrated higher values of phenolic compounds, vitamins and antioxidant capacity (Tables 1 and 2). Therefore, for the proof of concept, we exclusively used DG powder and its extract.

3.4.1. Rheological analyses

Fig. A2 represents the flow profile, frequency sweeps [markers filled in as storage modulus (G') and empty as loss modulus (G'')] and fluency compliance and recovery of the three mousse samples. The flow profile

curve (Fig. A2A) demonstrated a pseudoplastic profile for all samples, as indicated by the decrease in apparent viscosity with increasing shear rate. The flow profile index values obtained from the Herschel–Bulkley model adjustment were < 1 ($N < 1$), with values of 0.56 for the control sample, 0.56 for the MOP sample and 0.64 for the MOE sample. A thixotropic profile was also observed in the control sample, as evidenced by the formation of a hysteresis area between the ascending and descending curves, suggesting time dependence. The samples fitted to the Herschel–Bulkley model exhibited R^2 values > 99 %.

The MOP sample displayed a higher pseudoplastic profile, suggesting increased thixotropy (70.1 %). In contrast, the MOE sample showed a decrease (33.6 %) compared to the standard sample (36.2 %) (Fig. A2A). This profile could be attributed to the moisture content of the samples, as the presence of water from the aqueous extract could disturb the system. The higher thixotropy in the 2 % MOP sample may be attributed to the additional moisture required by the presence of leaf powder in the mousse while maintaining the appropriate solid–liquid ratio. The application of aqueous extract has been found to have a significant effect on the firmness, softness, overall texture and stability of mousses (Torres et al., 2018).

Fig. A2B shows that all mousse samples exhibited a gel-like structure, as the G' curve was consistently higher than the G'' curve. This finding is consistent with another study (Gomez-Betancur et al., 2020), which investigated the viscoelastic profile of mousse with the addition of concentrated protein powder. The MOE sample (G' : 7307.5 Pa and G'' : 2306.3 Pa) showed similar frequency sweep results to the standard sample (G' : 8408.4 Pa and G'' : 2412 Pa).

The viscoelastic profiles of the mousses are depicted in Fig. A2C, suggesting a partial recovery upon the removal of applied stress (Gomez-Betancur et al., 2020). Notably, all samples exhibited significant recovery values, with the MOP sample showing a recovery of 16.2 %, the control sample at 14.4 % and the MOE sample at 11.2 %. These findings suggest that the elastic component of the mousses predominated in all cases.

3.4.2. Texture profile analysis

The texture profile was used to distinguish differences in the texture properties of the mousses, as outlined in Table 3.

The texture of chocolate mousses can be evaluated using various attributes that capture different aspects of mastication. For instance, hardness and adhesiveness measure the force required to compress the mousse and its ability to stick to the teeth, respectively. Springiness assesses how well the mousse regains its original shape after being pressed or bitten, whereas cohesiveness determines its ability to hold together during chewing. Gumminess quantifies the chewing force needed to break the mousse into smaller pieces, whereas chewiness indicates the number of chews required before swallowing. Finally, resilience gauges how quickly the mousse returns to its original shape after deformation. These descriptors provide a comprehensive understanding of the mousse's texture and the sensory experience it offers.

The addition of both the powder and the extract did not result in significant treatment effects ($p < 0.05$), with distinct impacts observed in each sample. Notably, there were significant decreases in hardness, adhesiveness, springiness, gumminess and chewiness, suggesting that the texture was altered by the addition of the powder and extract. However, there was a slightly smaller difference observed in cohesiveness and resilience between the samples. These findings highlight the influence of the added powder and extract on the texture attributes of the samples, with notable reductions in some key parameters associated with mastication. This reduction is related to the compositional properties of the preparations and chemical interactions that influence the viscosity (Fig. A2) of the mousse.

The observed effects can be attributed to the interaction between phenolic compounds from moringa leaves and proteins from the milk during the preparation of the chocolate mousse. Previous studies have demonstrated that the solubility of casein, a key protein in milk, is a

crucial prerequisite for its functional performance in food and beverages (L. Chen et al., 2022). Phenolic compounds have been reported to influence the hydrophilic and hydrophobic properties and aggregation state of proteins, affecting their solubility. Phenolic compounds can both increase and decrease protein solubility by enhancing hydrophilicity and accelerating cross-linking and aggregation, respectively. The degree of aggregation is influenced by the structure of phenolic compounds, which, as demonstrated in Table 1, have the highest content in sample DG.

Proteins, due to their amphiphilic nature characterised by both polar and nonpolar amino acid residues, can function as emulsifiers by adsorbing at the oil/water interface, forming stable films and stabilising dispersions (Aryee et al., 2018). The emulsifying properties of proteins can be affected by changes in their spatial structure. Protein emulsifying activity is closely associated with their structural flexibility, with highly flexible proteins demonstrating better emulsifying activity as they easily unfold and rearrange their amino acid residues to absorb at the oil/water interface. In contrast, proteins with low structural flexibility are less likely to unfold and form films around dispersed oil droplets (Aryee et al., 2018, L. Chen et al., 2022).

The observed results in Fig. A2 align with the effects of adding the powder, which leads to increased plasticity and decreased viscosity of the mousse. These changes can be attributed to the presence of phenolic compounds, although their availability may be limited due to their entrapment within the matrix structure. However, the addition of the aqueous extract enhances the availability of phenolic compounds, facilitating their interaction with the milk casein. The foaming properties of casein, which involve the formation of stable air cells, significantly contribute to the overall texture and structure of the mousse (X. Chen et al., 2022). This is particularly important in the production of various food products based on milk, as it affects the stability of the foam.

The stability of foams is a complex phenomenon influenced by factors such as surface tension, bulk viscosity, surface rheological properties and surface forces. Additionally, the structure and mechanical properties of the film surrounding the air bubbles play a crucial role in foam stability (X. Chen et al., 2022). By modulating these factors, the presence of phenolic compounds and their interaction with milk casein can impact the stability and texture of the mousse. These findings highlight the intricate interplay between the ingredients and their effects on foam stability, ultimately influencing the overall sensory experience and quality of the chocolate mousse.

3.4.3. Sensory acceptability profile

The sensory evaluation allows for a comprehensive understanding of how consumers perceive the product, enabling the identification of strengths and areas for improvement. By considering the preferences of the target audience, product developers can make informed decisions to enhance the sensory characteristics and overall appeal of the chocolate mousse. This information is valuable in ensuring that the product meets consumer expectations and achieves a high level of acceptability in the market. Fig. 3A, B and C show the mousse samples used in this work. The sensory attributes evaluated through acceptance testing are graphically represented in Fig. 3D. The results indicate differences among the sensory properties of the samples. Overall, the control sample received the highest scores for all sensory properties.

The results of the sensory attributes tested in this study are presented in Fig. 3D, revealing variations across all five attributes. It is common in descriptive analysis panels for judges to utilise different parts of the scale or not fully use the entire scale when evaluating samples, leading to such variations. The reproducibility of the panel was confirmed, as there were no significant differences among repetitions for any of the evaluated attributes. The colour of the three formulations remained consistent, suggesting that the fortification process did not affect the colour of the mousse. Regarding the MOP sample, the results were similar to the control mousse in all aspects, except for aroma and flavour. In contrast,

the MOE sample exhibited significant differences in all aspects when compared to the control, except for colour. Overall, the general acceptance demonstrated a remarkable resemblance to the non-fortified product, with general acceptance levels of 93 % and 88 %, respectively.

4. Conclusions

This study emphasises the higher chemical value of DG *M. oleifera* leaves, characterised by a more favourable main composition, notably in terms of protein, fibre and mineral content. Consequently, its extract exhibited the highest concentrations of phenolic compounds, vitamins and antioxidant capacity. Thus, the mousses exclusively incorporated the DG powder and its extract, taking advantage of its enhanced nutritional profile and potential health benefits.

In the rheology analysis, all samples displayed a pseudoplastic profile, suggesting increased plasticity and decreased viscosity of the mousse. These changes can be attributed to the presence of phenolic compounds, although their availability may be limited due to entrapment within the matrix structure. However, the addition of the aqueous extract enhances the availability of phenolic compounds, facilitating their interaction with milk casein. The addition of the powder and extract significantly affected the texture attributes of the mousses, resulting in decreased hardness, adhesiveness, springiness, gumminess and chewiness, with minor differences in cohesiveness and resilience. Regarding sensory evaluation, samples containing 2 % MOP and 2 % MOE demonstrated a remarkable resemblance to the non-fortified product, with general acceptance levels of 93 % and 88 %, respectively.

CRedit authorship contribution statement

Olívia J.S. Gomes: Writing – review & editing, Writing – original draft, Investigation. **Anabela Leitão:** Writing – review & editing, Investigation. **Marisa C. Gaspar:** Validation, Investigation. **Carla Vitorino:** Validation, Investigation. **João J.S. Sousa:** Writing – review & editing, Validation. **Hermínio C. de Sousa:** Writing – review & editing, Resources. **Mara E.M. Braga:** Writing – review & editing, Writing – original draft, Supervision, Investigation. **Licínio M. Gando-Ferreira:** Writing – review & editing, Supervision, Funding acquisition, Conceptualization.

Declaration of competing interest

The authors declare that they have no known competing financial interests or personal relationships that could have appeared to influence the work reported in this paper.

Data availability

No data was used for the research described in the article.

Acknowledgements

This work was conducted under the Project MORfood (Ref. 541163254/2019): *Microencapsulation of Moringa oleifera extracts and their application in functional foods to mitigate child malnutrition in developing countries*, funded by the Foundation for Science and Technology (FCT) and Aga Khan Development Network, the Strategic Projects FCT-MEC of the Chemical Process Engineering and Forest Products Research Centre (CIEPQPF): UIDB/04539/2020 and UIDP/04539/2020, ciT-echCare: UIDB/05704/2020 and UIDP/05704/2020 and Coimbra Chemistry Center (CQC) is supported by FCT through the project UID/QUI/00313/2020.

Appendix A

See Figs. A1-A2.

See Table A1–A3.

References

- Abera, T., Tamtam, M. R., Koutavarapu, R., & Shim, J. (2022). Low-cost production and healthy preservation of malt drink using Melkassa-7 and Moringa oleifera leaf extract. *International Journal of Gastronomy and Food Science*, 29, Article 100568. <https://doi.org/10.1016/J.IJGFS.2022.100568>
- Adebayo, A. G., Akintoye, H. A., Shokalu, A. O., & Olatunji, M. T. (2017). *Soil chemical properties and growth response of Moringa oleifera to different sources and rates of organic and NPK fertilizers*. 10.1007/s40093-017-0175-5.
- Almeida, P. V., Rodrigues, R. P., Gaspar, M. C., Braga, M. E. M., & Quina, M. J. (2021). Integrated management of residues from tomato production: Recovery of value-added compounds and biogas production in the biorefinery context. *Journal of Environmental Management*, 299, Article 113505. <https://doi.org/10.1016/j.jenvman.2021.113505>
- AOAC International, Horwitz, W., & Latimer, G. W. (2010). *Official methods of analysis of AOAC International*. <https://www.worldcat.org/title/649275444>.
- APHA, AWWA & WEF (2023). *Standard Methods for the Examination of Water and Wastewater*. 24th ed., Eds. Lipps WC, Braun-Howland EB, Baxter TE. APHA Press, Washington.
- Aryee, A. N. A., Agyei, D., & Udenigwe, C. C. (2018). Impact of processing on the chemistry and functionality of food proteins. *Proteins in Food Processing, Second Edition*, 27–45. <https://doi.org/10.1016/B978-0-08-100722-8.00003-6>
- Bae, J., Kim, N., Shin, Y., Kim, S.-Y., & Kim, Y.-J. (2020). Activity of catechins and their applications. *Biomedical Dermatology 2020 4:1*, 4(1), 1–10. 10.1186/S41702-020-0057-8.
- Brar, S., Haugh, C., Robertson, N., Patrick, J., Owuor, M., Waterman, C., George, J., Fuchs Iii, J., Suzanna, J., Attia, L., & Attia, S. L. (2022). *The impact of Moringa oleifera leaf supplementation on human and animal nutrition, growth, and milk production: A systematic review*. 10.1002/ptr.7415.
- Bullard, J. W., Jin, Q., & Snyder, K. A. (2021). How do specific surface area and particle size distribution change when granular media dissolve? *Chemical Engineering Journal*, 406, Article 127098. <https://doi.org/10.1016/J.CEJ.2020.127098>
- Chen, L., Chen, N., He, Q., Sun, Q., Gao, M. R., & Zeng, W. C. (2022). Effects of different phenolic compounds on the interfacial behaviour of casein and the action mechanism. *Food Research International (Ottawa, Ont.)*, 162(Pt. B). <https://doi.org/10.1016/J.FOODRES.2022.112110>
- Chen, X., Chen, K., Cheng, H., & Liang, L. (2022). Soluble Aggregates of Myofibrillar Proteins Engineered by Gallic Acid: Colloidal Structure and Resistance to In Vitro Gastric Digestion. *Journal of Agricultural and Food Chemistry*, 70(13), 4066–4075. <https://doi.org/10.1021/acs.jafc.1c05840>
- Garai, L. (2017). Improving HPLC Analysis of Vitamin A and E: Use of Statistical Experimental Design. *Procedia Computer Science*, 108, 1500–1511. <https://doi.org/10.1016/J.PROCS.2017.05.177>
- Gomez-Betancur, A. M., Carmona-Tamayo, R., Jaimes-Jaimes, J., Casanova-Yepes, H., & Torres-Oquendo, J. D. (2020). Optimisation of yogurt mousse dairy protein levels: A rheological, sensory, and microstructural study. *International Food Research Journal*, 27(6), 1076–1086.
- Ia, S. (2021). Effect of dry shredded Moringa oleifera leaves and vitamin C on the physicochemical properties of the dough and bread Sengev IA, Agbanyi MM and Sule S. ~ 35 ~ *Journal of Current Research in Food Science*, 2(1). www.foodresearchjournal.com.
- Imdad, A., Mayo-Wilson, E., Haykal, M. R., Regan, A., Sidhu, J., Smith, A., & Bhutta, Z. A. (2022). Vitamin A supplementation for preventing morbidity and mortality in children from six months to five years of age. *The Cochrane Database of Systematic Reviews*, 2022(3). <https://doi.org/10.1002/14651858.CD008524.PUB4>
- Krakowska-Sieprawska, A., Kielbasa, A., Rafińska, K., Ligor, M., & Buszewski, B. (2022). Modern Methods of Pre-Treatment of Plant Material for the Extraction of Bioactive Compounds. *Molecules*, 27(3). <https://doi.org/10.3390/MOLECULES27030730>
- León-Félix, J., Angulo-Escalante, M. A., & Dorado, R. G. (2017). Nutritional and phenolic characterization of moringa Oleifera leaves grown in Sinaloa. *México*. <https://www.researchgate.net/publication/315044990>.
- Lobato-Calleros, C., Ramírez-Santiago, C., Vernon-Carter, E. J., & Alvarez-Ramirez, J. (2014). Impact of native and chemically modified starches addition as fat replacers in the viscoelasticity of reduced-fat stirred yogurt. *Journal of Food Engineering*, 131, 110–115. <https://doi.org/10.1016/J.JFOODENG.2014.01.019>
- Peñalver, R., Martínez-zamora, L., Lorenzo, J. M., Ros, G., & Nieto, G. (2022). Nutritional and Antioxidant Properties of Moringa oleifera Leaves in Functional Foods. *Foods*, 11(8). <https://doi.org/10.3390/FOODS11081107>
- Pérez-Patricio, M., Camas-Anzueto, J. L., Sanchez-Alegria, A., Aguilar-González, A., Gutiérrez-Miceli, F., Escobar-Gómez, E., Voisin, Y., Rios-Rojas, C., & Grajales-Coutiño, R. (2018). Optical Method for Estimating the Chlorophyll Contents in Plant Leaves. *Sensors (Basel, Switzerland)*, 18(2). <https://doi.org/10.3390/S18020650>
- Platzer, M., Kiese, S., Tybussek, T., Herfellner, T., Schneider, F., Schweiggert-Weisz, U., & Eisner, P. (2022). Radical Scavenging Mechanisms of Phenolic Compounds: A Quantitative Structure-Property Relationship (QSPR) Study. *Frontiers in Nutrition*, 9, Article 882458. <https://doi.org/10.3389/FNUT.2022.882458/BIBTEX>
- Pollini, L., Tringaniello, C., Ianni, F., Blasi, F., Manes, J., & Cossignani, L. (2020). Impact of Ultrasound Extraction Parameters on the Antioxidant Properties of Moringa Oleifera Leaves. *Antioxidants 2020, Vol. 9, Page 277*, 9(4), 277. 10.3390/ANTIOX9040277.
- Pueyo, M., Rauret, G., Lück, D., Yli-Halla, M., Muntau, H., Quevauviller, P., & López-Sánchez, J. F. (2001). Certification of the extractable contents of Cd, Cr, Cu, Ni, Pb and Zn in a freshwater sediment following a collaboratively tested and optimised three-step sequential extraction procedure. *Journal of Environmental Monitoring : JEM*, 3(2), 243–250. <https://doi.org/10.1039/B010235K>
- Rocchetti, G., Pagnossa, J. P., Blasi, F., Cossignani, L., Hilsdorf Piccoli, R., Zengin, G., Montesano, D., Cocconcelli, P. S., & Lucini, L. (2020). Phenolic profiling and in vitro bioactivity of Moringa oleifera leaves as affected by different extraction solvents. *Food Research International*, 127, Article 108712. <https://doi.org/10.1016/J.FOODRES.2019.108712>
- Sah, B. N. P., Vasiljevic, T., McKechnie, S., & Donkor, O. N. (2016). Physicochemical, textural and rheological properties of probiotic yogurt fortified with fibre-rich pineapple peel powder during refrigerated storage. *LWT - Food Science and Technology*, 65, 978–986. <https://doi.org/10.1016/J.LWT.2015.09.027>
- Seal, T., Chaudhuri, K., & Pillai, B. (2019). Simultaneous estimation of water soluble vitamin by high performance liquid chromatography (HPLC) method in five wild edible plants consumed by the tribal people of North-Eastern region in India. *Journal of Pharmacognosy and Phytochemistry*, 8(6), 2393–2398.
- Soukoulis, C., Rontogianni, E., & Tzia, C. (2010). Contribution of thermal, rheological and physical measurements to the determination of sensorially perceived quality of ice cream containing bulk sweeteners. *Journal of Food Engineering*, 100(4), 634–641. <https://doi.org/10.1016/J.JFOODENG.2010.05.012>
- Sultana, S. (2020). Nutritional and functional properties of Moringa oleifera. *Metabolism Open*, 8, Article 100061. <https://doi.org/10.1016/J.METOP.2020.100061>
- Teixeira, P. C., Donagemma, G. K., Fontana, A., & Teixeira, W. G. (2017). *Manual de métodos de análise de solo*. <https://www.embrapa.br>.
- Torres, I. C., Amigo, J. M., Knudsen, J. C., Tolkach, A., Mikkelsen, B.Ø., & Ipsen, R. (2018). Rheology and microstructure of low-fat yogurt produced with whey protein microparticles as fat replacer. *International Dairy Journal*, 81, 62–71. <https://doi.org/10.1016/J.IDAIRYJ.2018.01.004>
- Trigo, C., Castelló, M. L., & Ortolá, M. D. (2023). Potentiality of Moringa oleifera as a Nutritive Ingredient in Different Food Matrices. *Plant Foods for Human Nutrition (Dordrecht, Netherlands)*, 78(1), 25. <https://doi.org/10.1007/S11130-022-01023-9>
- UNICEF-WHO-The World Bank. (2023). *Joint Child Malnutrition Estimates (JME) — Levels and Trends — 2023 edition*. <https://data.unicef.org/resources/jme-report-2023/>.
- Vieitez, I., Maceiras, L., Jachmanián, I., & Alborés, S. (2018). Antioxidant and antibacterial activity of different extracts from herbs obtained by maceration or supercritical technology. *Journal of Supercritical Fluids*, 133, 58–64. <https://doi.org/10.1016/J.SUPFLU.2017.09.025>
- Vitorino, C., Alves, F. E., Antunes, F. E., Sousa, J. J., & Pais, A. A. C. C. (2013). Design of a dual nanostructured lipid carrier formulation based on physicochemical, rheological, and mechanical properties. *Journal of Nanoparticle Research*, 15(10), 1–14. <https://doi.org/10.1007/S11051-013-1993-7/FIGURES/5>
- Vonghirundecha, P., Chusri, S., Meunprasertdee, P., & Kaewmanee, T. (2022). Microencapsulated functional ingredients from a Moringa oleifera leaf polyphenol-rich extract: Characterization, antioxidant properties, in vitro simulated digestion, and storage stability. *LWT*, 154, Article 112820. <https://doi.org/10.1016/J.LWT.2021.112820>
- Xinyue Su, Guanzheng Lu, Liang Ye, Ruyi Shi, Maomao Zhu, Xinming Yu, Zhiyong Li, Xiaobin Jia, & Liang Feng. (2023). Moringa oleifera Lam.: a comprehensive review on active components, health benefits and application. *RSC Advances*, 13(35), 24353–24384. 10.1039/D3RA03584K.
- Yang, M., Tao, L., Kang, X.-R., Wang, Z.-L., Su, L.-Y., Li, L.-F., Gu, F., Zhao, C.-C., Sheng, J., & Tian, Y. (2023). Moringa oleifera Lam. leaves as new raw food material: A review of its nutritional composition, functional properties, and comprehensive application. *Trends in Food Science & Technology*, 138, 399–416. <https://doi.org/10.1016/J.TIFS.2023.05.013>
- Zhang, T., Jeong, C. H., Cheng, W. N., Bae, H., Seo, H. G., Petriello, M. C., & Han, S. G. (2019). Moringa extract enhances the fermentative, textural, and bioactive properties of yogurt. *LWT*, 101, 276–284. <https://doi.org/10.1016/J.LWT.2018.11.010>
- Zhang, Y., Liang, K., Wang, J., Wang, A., Pandiselvam, R., & Zhu, H. (2022). Evaluation of particle size on the physicochemical properties of Moringa oleifera Lam. stem powder. *Quality Assurance and Safety of Crops & Foods*, 14(SP1), 1–11. 10.15586/QAS.V14SP1.1123.
- Zungu, N., van Onselen, A., Kolanisi, U., & Siwela, M. (2020). Assessing the nutritional composition and consumer acceptability of Moringa oleifera leaf powder (MOLP)-based snacks for improving food and nutrition security of children. *South African Journal of Botany*, 129, 283–290. <https://doi.org/10.1016/J.SAJB.2019.07.048>